

1 **Temporary stratification promotes large greenhouse gas emissions in a shallow eutrophic lake**

2 Thomas A Davidson^{1,2}, Martin Søndergaard^{1,2,3}, Joachim Audet^{1,2}, Eti Levi¹, Chiara Esposito^{1,2}, Tuba
3 Bucak Onay¹, Anders Nielsen^{1,4}.

4

5 ¹ Lake Ecology, Department of Ecoscience, Aarhus University, Denmark

6 ² WATEC Aarhus University Centre for Water Technology, Aarhus University, Denmark

7 ³ Sino-Danish Centre for Education and Research (SDC), Beijing, China

8 ⁴ WaterITech Aps, Døjsøvej 1, 8660 Skanderborg, Denmark

9 Corresponding author: Thomas A Davidson, Department of Ecoscience, Aarhus University, C. F. Møllers

10 Alle 4-6, DK-8000 Aarhus C, Denmark, e-mail: thd@ecos.au.dk

11

12

13

14

15

16 **Abstract**

17 Shallow lakes and ponds undergo frequent temporary thermal stratification. How this affects greenhouse
18 gas (GHG) emissions is moot, with both increased and reduced GHG emissions hypothesised. Here,
19 weekly estimation of GHG emissions, over growing season from May to September, were combined with
20 temperature and oxygen profiles of an 11 hectare temperate shallow lake to investigate how thermal
21 stratification shapes GHG emissions. There were three main stratification periods with profound anoxia
22 occurring in the bottom waters upon isolation from the atmosphere. Average diffusive emissions of
23 methane (CH₄) and nitrous oxide (N₂O) were larger and more variable in the stratified phase, whereas
24 carbon dioxide (CO₂) was on average lower, though these differences were not statistically significant. In
25 contrast, there was a significant, order of magnitude, increase in CH₄ ebullition in the stratified phase.
26 Furthermore, at the end of the period of stratification, there was a large efflux of CH₄ and CO₂ as the lake
27 mixed. Two relatively isolated turnover events were estimated to have released the majority of the CH₄
28 emitted between May and September. These results demonstrate how stratification patterns can shape
29 GHG emissions and highlight the role of turnover emissions and the need for high frequency
30 measurements of GHG emission which are required to accurately characterise emissions, particularly
31 from temporarily stratifying lakes.

32

33

34 Keywords: Climate change; lake stratification; methane; carbon dioxide; nitrous oxide; climate
35 feedbacks

36

1. Introduction

Fresh waters are key sites for the processing of greenhouse gases (GHG), methane (CH₄), carbon dioxide (CO₂) and nitrous oxide (N₂O). Shallow lakes, in particular, have been identified as hot spots of CH₄ release, particularly when ebullition is taken into account (Davidson et al., 2018; Aben et al., 2017). The certainty that fresh waters are large emitters of GHGs contrasts with the uncertainties associated with the quantities emitted and this is in large part due to historical paucity of measurements (Cole, 2013). [A recent study identified the highly variable emissions from lakes and ponds](#) (Rosentreter et al., 2021). Whilst different morphometric features and chlorophyll-a explained some of the emission patterns (Deemer and Holgerson, 2021), it is also clear that a dearth of measurement combined with these highly variable emissions makes determining the drivers and controls of those emissions a challenge, which in turn makes predicting future emissions difficult.

The current and future effects of climate change on lakes in general and on their GHG emissions are relevant questions as there is potential for positive feedbacks and synergies with other human impacts such as eutrophication (Davidson et al., 2018; Beaulieu et al., 2019; Delsontro et al., 2016; Meerhoff et al., 2022). Taking a broad metabolic theory of ecology approach, temperature increases should promote methanogenesis and shift the balance from primary production to respiration increasing CO₂ emission at cellular and ecosystem scale (Yvon-Durocher et al., 2010). However, empirical and experimental data indicate that temperature is not the sole control of primary production and methanogenesis. In particular, eutrophication, and the promotion of large algal crop, has been associated with increased emissions of CH₄ and N₂O (Delsontro et al., 2016) both by diffusion and ebullition (Zhou et al., 2019). Furthermore, in what is globally the most abundant lake type, small shallow lakes, where macrophytes can colonise large areas of the lake bed, trophic state and the dominance of submerged plants or algae may be more important than temperature in shaping GHG dynamics (Davidson et al., 2015; Davidson et al., 2018; Bastviken et al., 2023).

62

63 Climate change effects on lakes are not limited to increases in average temperatures and lengthening of
64 the growing season. Increases in both the frequency and intensity of heat waves are predicted, which will
65 promote the warming of surface waters and in turn make permanent and temporary thermal stratification
66 of lakes more likely (Woolway and Merchant, 2019), even in lakes typically classified as non-stratifying
67 (Kirillin and Shatwell, 2016). A recent study Holgerson et al. (2022) identified stratification and mixing
68 patterns in small water bodies, with permanent summer stratification common and frequent mixing
69 occurring in larger standing waters (>4 ha) lakes. Such periods of stratification and mixing events are
70 likely to have profound effects on GHG dynamics. Emissions of gases, in particular CH₄, that accumulate
71 in the isolated bottom waters of a stratified lake, occurs upon mixing and can make very significant
72 contributions to cumulative emissions (Schubert et al., 2012). High-resolution studies of sites that
73 undergo temporary stratification are rare. Though Søndergaard et al. (2023b), recently showed how
74 stratification shapes patterns and processes across the entire ecosystem, including short term effects on
75 dissolved GHG concentration in bottom and surface waters. In terms of its effects on GHG dynamics,
76 there are potentially antagonistic processes at work in a stratified lake. On the one hand the ‘shield effect’
77 results in lower temperatures at the sediment surface slowing down metabolic processes that scale with
78 temperature, i.e. methanogenesis and mineralization of organic carbon (C), reducing emission and
79 promoting C burial. On the other hand, anoxia at the sediment surface may shift processes towards
80 fermentation, increasing the proportion and total amount of CH₄ produced and perhaps reducing C burial
81 (Bartosiewicz et al., 2019). Recent work combining empirical observations and models has suggested that
82 shielding effects are larger than the anoxia effects and that stratification, in general, increases C burial and
83 reduces GHG emissions (Bartosiewicz et al., 2015). The stratification induced isolation of bottom waters
84 was reported to lead to reduced ebullition of CH₄ and a shift to diffusive pathways (Bartosiewicz et al.,
85 2015). It might, however, be predicted that in shallow lakes stratification would lead to much larger CH₄
86 release as anoxic conditions would limit CH₄ oxidation by CH₄ oxidizing bacteria (MOBs) (Bastviken et
87 al., 2008). There may also be other factors with the potential to increase GHG emission, such as sediment

88 organic content and lake trophic status (Delsontro et al., 2016), which may interact with stratification
89 patterns in shaping GHG emissions.

90
91 In this study, we used data from a shallow lake with high frequency measurements of temperature profiles
92 combined with weekly measurements of dissolved gas concentrations in the surface and bottom waters
93 and continuous measurement of ebullitive emissions of CH₄ to track the effects of lake stratification on
94 GHG emissions. The key question was how ebullitive and diffusive fluxes of the key GHGs: CH₄, CO₂
95 and N₂O respond to temporary thermal stratification.

96

97 **2. Materials and methods.**

98 **2.1 Study site**

99 Ormstrup lake, located in Denmark (lat 56.326°, lon 9.639°) (Fig.1) (depth map with GHG sampling
100 locations), is an 11 ha, shallow lake (average depth 3.4 m), with a maximum depth of 5.5 m, and with a
101 relatively long hydraulic retention time (> 1 year). The lake is eutrophic with high TP and chlorophyll-a
102 (Table 1; Søndergaard et al., 2022) with very sparse occurrence of submerged plants.

103

104 **2.2 Depth profiling and high frequency measurements**

105 In June 2020, a Nexsens (NexSens Technology, Fairborn, OH, USA) CB-450 data buoy system
106 (https://www.nexsens.com/pdf/CB450_datasheet.pdf) was deployed at the deepest point of the lake
107 equipped with a Nexsens TS210 thermistor string https://www.nexsens.com/pdf/TS210_datasheet.pdf
108 with temperature nodes measuring at 4 levels; one sensor “in air”, ca. 5 cm above the water surface, (but
109 shielded from direct light), and three sensors at -1, -2, -3 meters, respectively relative to the water surface.
110 In addition two Aqua TROLL 500 (In-Situ, Fort Collins, CO, USA) multi-sondes were mounted near the
111 surface (-1.0 meters) and at deeper water depth (-3.8 meters). The near surface and deeper water sonde

112 were configured with sensors to measure dissolved oxygen (DO) and water temperature (Tw). The optical
113 sensors were calibrated according to manufacture guidelines and checked on a weekly basis.

114

115 The optical sensors of the Aqua TROLL 500 have a built-in wiper mechanism to clean sensor heads to
116 hamper bio-fouling. The wiper function was enabled to perform cleaning in sync with sensor
117 measurements, hence every 15 minutes. In addition, manual cleaning of sensor heads was done every
118 week, while routine manual field monitoring was carried out at the lake. Prior to the deployment of the
119 buoy, and as a validation exercise for the buoy data, weekly manual profiles of DO and Tw were collected
120 at the deepest point.

121

122 -Periods of stratification and depth of the thermocline were defined using the r package rlakeanalyzer
123 (Winslow et al., 2019) based on the density gradient of the water column from the weekly manual
124 profiling of the system. During periods of defined as stratified, there were partial mixing events where the
125 depth of the thermocline changed and there was some mixing of the sub epilimnetic water and the surface
126 waters, whilst the bottom waters below 3.5 metres remained undisturbed.

127

128 **2.3 Water chemistry**

129 Water samples for the analysis of Chlorophyll-a were collected weekly from the 20. April 2020 from
130 surface (-0.5 m) water at station 3 (Fig. (Søndergaard et al., 2005)). A volume of water ranging from (0.2
131 to 1 litre) was filtered and the GFC papers preserved for chlorophyll-a analysis, which were determined
132 spectrophotometrically after ethanol extraction (Jespersen and Christoffersen, 1987) and alkalinity was
133 measured weekly by gran titration (Søndergaard et al., 2005). Depth profiles of temperature, electrical
134 conductivity (EC) and dissolved oxygen (DO) were measured manually with an Aqua TROLL 500 probe
135 from every -0.5 or -1 m down to -5 m depth).

136

137 **2.4 Greenhouse gas sampling**

138 2.4.1 Dissolved concentration

139 Samples of dissolved concentrations of CH₄, CO₂ and N₂O were collected weekly from the 20. April 2020
140 from surface waters and weekly from surface and bottom water from the 26. May 2020 to the 13. October
141 2020. The samples were taken using head-space equilibration after (Mcauliffe, 1971), where 20 ml of
142 water was collected from just below the water surface and 20 ml of N₂ was introduced as a headspace in a
143 60-ml syringe and then shaken vigorously for one minute. The 20 ml headspace was then transferred to a
144 12-ml pre evacuated glass vial.

145
146 Gas concentrations in the headspace were determined on a dual-inlet Agilent 7890 GC system interfaced
147 with a CTC CombiPal autosampler (Agilent, Nærum, Denmark) (Petersen et al., 2012). For the GC,
148 certified CO₂, CH₄ and N₂O standards were used for calibration and validation. Aqueous concentrations in
149 N₂O, CH₄ and CO₂ were calculated from the headspace gas concentrations according to Henry's law and
150 using Henry's constant corrected for temperature and salinity (Weiss, 1974; Weiss and Price, 1980;
151 Wiesenburg and Guinasso, 1979). A recent study (Koschorreck et al., 2021) identified significant bias in
152 the estimate of CO₂ concentrations using headspace equilibration at lower concentrations. We applied their
153 correction using separately measured alkalinity as described in Koschorreck et al. (2021).

154 The fluxes of N₂O, CH₄ and CO₂ between the water and the overlying atmosphere were estimated as

$$155 \quad f_g = k_g(C_{wat,g} - C_{eq,g})$$

156 Where f_g is the flux of a specific gas g , k_g is the piston velocity of the gas and $C_{wat,g} - C_{eq,g}$ is the
157 gradient of concentration between the concentration of gas dissolved in the water ($C_{wat,g}$) and the
158 concentration of gas the water would have at equilibrium with the atmosphere ($C_{eq,g}$).

159 We calculated a gas transfer velocity k_{600} for each sampling occasion using the relationship based on
160 windspeed described in (Cole and Caraco, 1998).

161
162
163
164
165
166
167
168
169
170
171
172
173
174
175
176
177
178
179
180
181
182
183
184
185

$$k_{600} = 2.07 + 0.215U_{10}^{1.7}$$

U_{10} is the mean daily windspeed at 10m ($m s^{-1}$) obtained from the Danish meteorological institute (DMI;20x20 km grid data)

$$k_g = k_{600} \left(\frac{Sc_g}{600} \right)^x$$

Sc_g is the Schmidt number(Wanninkhof, 1992) of the specific gas g . We chose $x = -2/3$ as this factor is used for smooth liquid surface (Deacon, 1981).

Daily flux rates were calculated using linear interpolation of the weekly surface measurements from each of the sampling points. The diffusive surface water fluxes were calculated by taking an average of the daily flux rate from the 12. May 2020 to the 13. October 2020 for each location. Then an average of the 3 locations was multiplied by the area of the lake and the number of days covered by the study, here 126 days was chosen to match the period over which ebullition was measured.

The total content of the gases in the lake's bottom waters were calculated from the dissolved concentration of the gases multiplied by an estimate of the volume of the water in the hypolimnion. The volume of water in the hypolimnion was estimated from the lake profiles manually conducted on the day of sampling. The top of the hypolimnion was determined by the depth below which oxygen was less than $0.5 mg l^{-1}$. A detailed bathymetry of the lake allows the calculation of the area and therefore volume of water that lies below a given depth.

During the study period two major turnover events occurred, the process of lake turnover and full mixing can take a number of days, and the outgassing even longer. The oxygen data, from the buoy, indicated

186 that it can take up to four days and this provides time for CH₄ oxidation to occur (Søndergaard et al.,
187 2023b). In order to estimate the amount of CH₄ oxidised over the course of the multiple days of degassing
188 we directly measured CH₄ oxidation rates in the surface waters of the lake. This was done in June 2023 in
189 five locations [in this lake](#) using methods outlined in (Thottathil et al., 2019) where five water samples
190 from five different locations and each was incubated over 4 days with and the change in CH₄
191 concentration used to calculate oxidation rates. We used the minimum (0.267 μg CH₄-C l⁻¹ h⁻¹), mean
192 (0.44 μg CH₄-C l⁻¹ h⁻¹) and maximum (0.58 μg CH₄-C l⁻¹ h⁻¹) oxidation rates to estimate the range of CH₄
193 oxidation likely to have occurred over the course of the two main turnover events. Assuming that the
194 degassing took four days, these rates would consume between 2 and 8% of the CH₄ contained in the
195 hypolimnion. Using the mean oxidation value the turnover fluxes were reduced by 4.1% on the 30th of
196 June 2020 and by 6% for the 25th August 2022.

197

198 2.4.2 Ebullition

199 The ebullitive flux of CH₄ was estimated using a total of 40 floating chambers placed on 4 transects of 10
200 chambers each (Fig. 1). The chambers have a volume of 8 litre and a surface area of 0.075 m², similar to
201 those used by (Bastviken et al., 2015). As the existing literature indicated that ebullition is lower as water
202 depth increases (Wik et al., 2013) the transects were placed to maximise the measurement of the low end
203 of the depth gradient on the shallower slopes of the western end of the lake (Fig. 1). The average and
204 maximum depth of each transect was T1: 293 cm and 472 cm; T2: 181 cm and 267, T3: 223 cm and 300
205 cm and T4 166 cm and 220 cm. The chambers were set on the 14. May 2020 and sampled every two
206 weeks from that date, and on one occasion after one week until September 17th, which is a period of 127
207 days. Twenty ml of sample was taken from the floating chamber and injected into a pre-evacuated 12 ml
208 vial (exetainer, Labco). Gas concentrations were determined on the same GC than described above
209 (Petersen et al., 2012)

210 Ebullitive flux of CH₄ was estimated as:

211
$$\frac{p_{gas} \times Vol_{bub}}{t \times A}$$

212 Where p_{gas} is the concentration of CH₄ in the gas that was trapped, Vol_{bub} is the volume of the chamber
213 (i.e. 7L), t is the time during which the samples was collected and A is the area of chamber (i.e. 0.075 m²).
214 A portion of the CH₄ released via ebullition in the chamber will have re-dissolved in the water or might
215 leak through the chamber walls, thus underestimating the ebullitive flux. We have made a number of
216 measurements to constrain this error and to compare estimates based on static chambers with other
217 approaches. The result show that whilst static chambers underestimate ebullition, given the temporal
218 variability of ebullition, static chambers continually deployed provide a better estimate of average ebullition
219 than short term (24-48 hours) deployment using portable gas monitors or flushing chambers.

220
221 Therefore, whilst static chambers method cannot be said to accurately quantify CH₄ emissions, they can be
222 relied upon to compare differences in ebullition between time periods, with the caveat that they are always
223 an underestimate of actual ebullitive flux.

224
225 Total ebullitive flux from the lake was calculated by taking a mean of the emissions from each transect over
226 the 126 day period. Then taking an average of the means of four transects and multiplying this by the time
227 of deployment of the chambers in days, which was 126 days, and by the area of the lake. This gives a total
228 ebullitive flux of CH₄ for the lake over the period of measurement from May to mid-September.

229
230 The three different flux types, surface diffusion, ebullition and turnover emission were then converted in
231 comparable units of total lakes emissions (as g or kg of gas) over the studied period and also converted into
232 CO₂-equivalents using a conversion factor related to their 100 year global warming potential (GWP) of 28
233 for CH₄ and 265 for N₂O.

234
235 **2.5 Statistical methods**

236 To test for a significant difference among the emissions from the stratified and mixed phase we used
237 generalised least squares (GLS) with a variance function to account for heterogeneity of variance between
238 the phases. In the case of the ebullitive flux, as the collected phase often covered periods including both
239 mixed and stratified phases there were three categories, mixed, stratified and both mixed and stratified.
240 All analysis was carried out in R version 4.2.1 (R Development Core Team, 2022) and the GLS used the
241 package nlme (Pinheiro et al., 2014).

242

243 **3.0 Results**

244 **3.1 Lake physical and chemical characteristics**

245 Depth profiles measured weekly from April show that stratification was initiated by the 26. May 2020 this
246 may have broken down briefly and established again, visible in the temperature sensors for the buoy on
247 the 5. June 2020 (Fig. 2). There were then 12 days of mixing followed by stable period of stratification
248 with onset the 14. June 2020 and a duration of 16 days until a mixing event around the 30. June 2020. The
249 following two weeks had cooler water and a mixed water column, hereafter a ca. 6 day period of
250 stratification from the 15. to 21. July 2020. A mixed phase of two weeks then followed until stratification
251 reestablished on 4. August 2020 and persisted until the end of August, partial mixing is indicated by the
252 buoy data from the 21. August 2020, but the weekly manual profile to deeper water indicate that full
253 mixing did not occur until after the 25. August 2020. The effects of the stratification and mixing events on
254 the high frequency DO data measured at -3.8 m are clear, with rapid deoxygenation occurring after the
255 onset of stratification and oxic bottom waters returning when the lake mixed (Fig, 2). The pattern in
256 chlorophyll-a also follow, to some degree, those of stratification, with the exception of early spring.
257 Chlorophyll-a values were extremely high in spring peaking at the start of June 2020 and falling gradually
258 (Fig. 2). (Søndergaard et al., 2023b) During the periods of stratification chlorophyll biomass was lower,

259 and when a mixing event occurred the values increased, which is particularly evident in the July mixing
260 periods (Fig. 2).

261

262 **3.2 Concentrations of dissolved gases and fluxes from the surface waters.**

263 The concentrations of the dissolved gases showed great variation from near or below atmospheric
264 concentrations in some cases and up to an extremely high concentration (over 5 mg CH₄ C l⁻¹) in the
265 bottom waters on the 30. June 2020. There was some spatial heterogeneity in the surface waters, with the
266 more littoral locations showing the greatest variation and the highest values (Figs. 3,4,5). In particular the
267 most littoral zone, where the water was shallower around 1 m in depth, showed the highest values just
268 prior to, or coincident with, the stratification turnover. Table 2 shows the mean diffusive flux of each gas
269 over the sampling period along with the mean flux in mixed and stratified phases. For CO₂ there was a lot
270 of temporal variation in flux dynamics, though not a large difference between mixed and stratified phases
271 in terms of mean values (Table 2). There were some periods of CO₂ influx in spring and later summer and
272 these tended to coincide with the end of a mixed phase and the start of the stratification phase. Nitrous
273 oxide concentrations were generally low (Figs 4 & 5) with the lake being a source of N₂O in the spring
274 period and a sink or a very small source thereafter. The CH₄ concentration in the surface waters (Fig. 3)
275 and the calculated diffusive emissions are relatively low, but did increase in the stratification periods with
276 higher average values (Table 2 & Fig. 6). There was also some spatial variation with higher CO₂ and CH₄
277 diffusive emissions in the shallower sampling locations, both in stratified and mixed conditions (Fig. 6).

278

279 The most marked patterns in GHG concentration were evident in the bottom waters sampled at -4.5 m,
280 which accumulated to very large concentrations of CO₂ but particularly CH₄ in the periods of
281 stratification (Fig. 3 & 4). The ratio of CO₂ to CH₄ is illustrative in highlighting how stratification has
282 altered the biogeochemical processes in the hypolimnion with CH₄ production becoming more prevalent. .

283 For example on 30. June 2020 after 16 days of stratification the the ratio $\text{CO}_2:\text{CH}_4$ in the bottom waters
284 was 0.8, whereas 7 days later after the mixing event it was 187 at the same depth.

285

286 **3.3 Ebullitive fluxes**

287 The CH_4 bubble flux, presented here as mean values for each of the 4 transects, ranged from 0.303 to 81.1
288 $\text{mg CH}_4 \text{ C m}^{-2} \text{ d}^{-1}$ for the individual transect over the growing season measurement. There is a very clear,
289 statistically significant impact of stratification on the ebullitive efflux of CH_4 with stratified periods
290 showing significantly markedly higher levels of emission (Fig. 7 and Table 2). In addition, there was a
291 difference in average emissions among the different transects, with those with lower average water depth
292 (T2 & T4) having lower emission than the transects with chambers over deeper water (T1 & T3) (Fig. 7).

293 The samples collected from the chambers reflect two weeks of bubble and diffusion collection and the
294 quantification of the flux is therefore an average of the period of chamber deployment, which was two
295 weeks, or in one case a single week (Fig. 7). This two week period on occasion covered both stratified
296 and mixed phases and on these occasions efflux was intermediate between purely mixed and stratified
297 periods (Table 2 and Fig. 7).

298

299 **3.4 Total lake fluxes**

300 Scaling up the results to total flux of gases from the whole lake over the period of study and including the
301 estimated emissions from two turnover events show a very different effect of stratification on the balance
302 of types of emissions for the three gases. The majority of CH_4 emission (56%) result from the two short-
303 lived turnover events (Fig. 8), whereas their contribution to CO_2 and N_2O emission was 5% and 1%
304 respectively.

305

306 Fluxes of CO_2 and N_2O were mostly diffusive, which represented 95% of emissions of both gases.

307 Methane diffusive flux was 14% of total emission, whereas CH_4 ebullition was more than twice as much at

308 29% of total CH₄ emission. In terms of global warming potential CO₂ and CH₄ emission were
309 comparable, but the contribution of the turnover efflux was the dominant factor for CH₄ emissions.

310

311 **4. Discussion**

312 This study set out to assess the role of thermal stratification on the GHG dynamics in a lake undergoing
313 frequent but temporary stratification. We found that ~~T~~the emission of the three GHGs showed different
314 degrees of variation between the mixed and stratified phases. The largest and most significant variation
315 was in CH₄ ebullition (Table 2), whilst the difference in diffusive fluxes, though marked for CH₄ was not
316 significant. The mean of the total emissions from Ormstrup in the stratified phase (59.9 mg CH₄-C m⁻²
317 day⁻¹) corresponds relatively closely to the mean of the total emissions (ebullition plus diffusion) reported
318 for lakes in this size range (47 mg CH₄-C m⁻² day⁻¹) from a paper synthesising multiple studies
319 (Rosentreter et al., 2021). The mean emissions for the whole period (26.6 CH₄ -C m⁻² day⁻¹) were lower
320 than Rosentreter et al. (2021) but similar to other studies with mean emissions of 30.9, 20.7 and 22.7 CH₄
321 -C m⁻² day⁻¹ and were reported by Peacock et al. (2021), Sørensen et al. (2023) and Peacock et al. (2019)
322 respectively. Whereas the average CO₂ (504 mg CO₂-C m⁻² day⁻¹) at Ormstrup was lower than 993.5 mg
323 CO₂-C m⁻² day⁻¹ measured by Peacock et al. (2021) but higher than the 264.6 and 205.1 mg CO₂-C m⁻²
324 day⁻¹ measured by Sørensen et al. (2023) and Peacock et al. (2019) respectively. The different temporal
325 resolution and duration of these studies, eleven single day sampling from April to December (Peacock et
326 al., 2021), five days continuous sampling on one occasion in late September (Sørensen et al., 2023) and a single
327 early summer snapshot (Peacock et al., 2019) make direct comparison difficult. The data here do,
328 however, provide a clear answer to the question of how thermal stratification affects GHG dynamics in
329 shallow eutrophic lakes with an increase in total emissions (diffusion, ebullition and turnover) during the
330 stratified period (Table 2, Fig 9). Previous work, combining observations and modelling suggested the
331 opposite patterns (Bartosiewicz et al., 2019) as the shielding effect of the stratification results in cooler
332 bottom waters which reduces CH₄ production due to the process being temperature dependent

333 (Bartosiewicz et al., 2016). This strong shielding effect may apply in deeper lakes experiencing more
334 stable stratification, or less eutrophic lakes. The result here from a relatively shallow eutrophic lake,
335 indicate that temporary stratification causes increases in GHG emissions.

336

337 **4.1 Diffusive fluxes**

338 Diffusive emissions did not, on average, show a strong stratification effect (Table 2). In particular
339 variation in N₂O emissions did not match patterns of stratification, with emissions more directly related to
340 nitrate concentrations (Audet et al., 2020), as reflected by the fact the lake is a sink of N₂O in late summer
341 when nitrate was below detection limits for several weeks. There were peaks in emission of CH₄ and CO₂
342 at the end of stratification periods, particularly in the shallower water sampling points (Fig. 6). There
343 were periods of influx of CO₂, which coincided somewhat with periods of stratification, but the pattern
344 was not consistent as other factors, for example, chlorophyll-a concentration also play a role.

345

346 Littoral zones can have markedly different GHG dynamics to deeper zones due to shallower water having
347 lower pressure (Wik et al., 2013), less time for CH₄ oxidation (Bastviken et al., 2008) or abundant plants
348 which influence a range of biogeochemical processes (Davidson et al., 2018; Esposito et al., 2023). It is
349 therefore possible that littoral zone dynamics could cause these differences. However, the increase
350 occurred at all three sampling points at the end of June 2020, which indicates a lake-wide driver and the
351 peak may represent the start of mixing after stratification. Strong winds were measured on the 29th and
352 30th June 2020 (Søndergaard et al., 2023b) coincident with these increased littoral emissions. These
353 winds would have caused lateral movement of the surface water causing an upwelling of bottom water,
354 rich in CH₄ and CO₂, in the littoral margins at the opposite end of the lake. Thus, whilst we do not have
355 direct evidence it seems more likely that these increased emissions in the littoral zone were driven, at least
356 in part, by the upwelling of GHG rich bottom waters.

357

358

359 **4.2 Ebullitive fluxes**

360 In contrast to the diffusive flux, the ebullitive emission of CH₄ shows a very clear response to
361 stratification with an order of magnitude difference in emissions between periods where the sampling
362 reflected purely mixed or stratified periods (Table 2 & Fig. 7). The two-week resolution of the sampling
363 meant that some samples covered both stratified and mixed phases and these samples had intermediate
364 fluxes, as they cover both low (mixed) and high emission (stratified) periods. The spatial variation in
365 ebullition is also illustrative of the impacts of stratification and the role of anoxia in shaping CH₄ fluxes.
366 The two transects with the largest mean and maximum depths (T1 and T3) had the largest emissions, with
367 the deeper of the two (T1) having the highest emissions and showing the largest relative increase during
368 the stratification phases. This pattern is different to that found some other studies where bubble emissions
369 were larger in shallower water (Wik et al., 2013), although in this, and another study (Sø et al., 2023),
370 there was an increase in bubble flux in deeper water in late summer. The deeper water at Ormstrup
371 experienced anoxia early in season resulting in locations with deeper water having higher ebullition rates
372 than shallower areas. This is at odds with ideas stemming from the metabolic theory of ecology stating
373 that temperature (Yvon-Durocher et al., 2014) in particular at the sediment surface (Bartosiewicz et al.,
374 2019) can be used to predict CH₄ efflux. Whilst CH₄ production is temperature dependent at the cellular
375 level, CH₄ emissions were rather independent of the sediment temperature, for example in the first two
376 weeks of July 2020 emissions were low and the sediment surface temperature was relatively high. Thus,
377 temperature alone is a poor predictor of ecosystem scale CH₄ emissions.

378

379 It should be noted that the methods used to estimate bubble flux here, where floating chambers are
380 sampled every two weeks is a “less than perfect method”, which in nearly all cases will underestimate
381 ebullitive flux. Logistical and financial constraints make continual sampling difficult and here we
382 balanced these constraints against the greater time required to apply more accurate methods, such as

383 bubble traps (Wik et al., 2013), automatic flushing chambers (Bastviken et al., 2015). ~~Such is the~~
384 ~~variability of bubble flux in space and time that sampling campaigns covering days or weeks would~~
385 ~~potentially give an even more inaccurate picture of emissions than the method used here.~~ Such is the
386 variability of bubble flux in space and time that using measurement from a shorter period of 1-2 days can
387 result in a larger error in estimation of emissions than results from the longer term deployment of a static
388 chamber (see supplementary materials 1 and 2). The results in figure 7 show that sampling a single week
389 a year or even more regular monthly sampling of a shorter duration would be unlikely to accurately
390 characterise ebullition. Bubble traps have been used on longer terms but in eutrophic systems they can
391 suffer extensive biofouling which can impede their use. Thus, the continuous monitoring of ebullition
392 using static chamber with known biases was deemed the least worst method available, but we
393 acknowledge that ebullitive emissions are underestimated. We further acknowledge that this approach of
394 static chambers should, where possible, be replaced by other methods to estimate ebullition, such as
395 automatic flushing chambers. It is difficult to compare the mean values of emission with other studies as
396 there are different scales of measurement both in space and time. However, comparing the values for
397 ebullition recorded here with other longer-term studies carried out in lakes using bubble traps (Burke et
398 al., 2019; Delsontro et al., 2016), shows higher values recorded at Ormstrup lake compared with other
399 lakes, but lower values that have been measured in ponds (Ray and Holgerson, 2023; Delsontro et al.,
400 2016), the latter being known to have higher emissions of CH₄ (Holgerson and Raymond, 2016).

401

402 4.3 Turnover fluxes

403 In addition to the diffusive and ebullitive emissions, the turnover flux, which consists of the gases
404 accumulated in the hypolimnion being released on turnover, was also estimated, with a correction of CH₄
405 oxidation applied. There were two major turnover events at the end of June and in late in August 2020,
406 which were preceded by 16 and 22 days of stratification, respectively. It was not possible to directly-
407 measure turnover flux, as they are relatively discrete events where the efflux likely occurs over the course

408 of a few hours, or a few days (Søndergaard et al., 2023b). Thus, the efflux estimation is based on a series
409 of assumptions and thus must be treated with caution. Notwithstanding this uncertainty, we can be
410 confident the turnover flux represents a very large proportion of the total emission of CH₄ emissions from
411 Ormstrup Lake over the growing season. We estimate it contributed more than 50 % of growing season
412 CH₄ emissions and 5 % of CO₂ emissions. This highlights a very significant, and difficult to measure,
413 contribution to GHG emissions from lakes undergoing temporary stratification, which are among the
414 most common lake type in Denmark (Søndergaard et al., 2023a).

415

416 **4.1 Stratification effects**

417 The results here suggest that GHG dynamics were driven both directly and indirectly by the stratification
418 patterns and the anoxia it induced in the bottom waters. At Ormstrup Lake the thermal stratification of the
419 water column quickly led to anoxia, with only a matter of hours to days for the oxygen to be consumed
420 once the bottom waters were isolated (Fig. 2). The ratios of CO₂:CH₄ evidence how this promotes CH₄
421 over CO₂ production in the stratification phase (see Fig 9). In addition to promoting CH₄ production such
422 conditions would preclude, or severely limit, oxic CH₄ oxidation, which has the potential to consume a
423 large proportion of CH₄ produced in the anoxic sediments (Bastviken et al., 2008), though anoxic
424 consumption of CH₄ can still occur (Blees et al., 2014). The raw emission data do not provide any direct
425 information on the balance of production versus oxidation, but the CO₂:CH₄ suggest there was marked
426 shift to conditions where methanogenesis was the dominant process and there was reduced CO₂
427 production. Studies have shown that CH₄ oxidation can consume large proportions of the CH₄ produced
428 under hypoxia (Saarela et al., 2019) and it is possible that there is intense CH₄ oxidation occurring at the
429 thermocline during the periods of stratification at Ormstrup lake , but this was not directly measured at the
430 lake. In addition to the more direct effects of anoxia there may be some indirect effects of the patterns of
431 stratification and mixing that promote greater GHG emissions. Søndergaard et al. (2023b) recently
432 reported how nutrient dynamics at Ormstrup Lake were altered by the lake stratification and full details

433 can be found there, of relevance here is the impact on chlorophyll-a which saw a large spring peak after
434 which the abundance tracked the stratification and mixing regime, with a lag time. There was a general
435 reduction, or at least no increase as the stratification period progressed, perhaps due to nutrient limitation
436 in the epilimnion. Upon mixing there was generally an increase in chlorophyll-a, though the weekly
437 sampling resolution makes this difficult to assess. Chlorophyll-a and the labile dissolved organic carbon
438 (DOC) that result from abundant chlorophyll-a have been shown to be associated with higher diffusive
439 and ebullitive CH₄ emissions (Davidson et al., 2015; Beaulieu et al., 2019; West et al., 2012; Zhou et al.,
440 2019). It is not possible to say here whether a stable summer long stratification would have led to
441 decreased chlorophyll-a as nutrients became limiting due to their isolation in the bottom waters and
442 reliable high frequency chlorophyll-a data are required to convincingly demonstrate this phenomenon.
443 Notwithstanding these uncertainties it may be the case that the temporary stratification, interspersed with
444 mixing events, observed here represents a ‘sweet spot’ providing both the resources, i.e. chlorophyll-a and
445 the labile DOC it produces, and optimal conditions (anoxia) for CH₄ production.

446

447 Predicting climate change effects on GHG emissions in a future warmer world is not straightforward, as
448 there are multiple interacting drivers which combine to shape the GHG emissions of lakes. However, this
449 study suggests that temporary stratification, which is increasingly recognised as prevalent in ponds and
450 shallow lakes (Holgerson et al., 2022) and is likely to become more common with continued climate
451 change impacts (Woolway and Merchant, 2019) is likely to increase GHG emissions. This will be
452 particularly the case in more eutrophic systems where abundance algal derived dissolved organic matter
453 can fuel CH₄ production (Zhou et al., 2019).

454

455 The combination of high frequency data on water temperature and dissolved oxygen combined with
456 weekly measurements of GHGs increase the reliability of the findings presented here. Up until relatively
457 recently it has been assumed that for shallow lakes, such as Ormstrup lake, stratification is not an
458 important feature. Sampling has therefore focused on the surface layers of water bodies, using dissolved

459 concentrations of gases or floating chambers to characterise flux, e.g. (Davidson et al., 2015; Audet et al.,
460 2020; Peacock et al., 2021). Thus, most studies have overlooked bottom waters and do not have the
461 temporal resolution required to capture turnover flux emissions from surface measurements. Furthermore,
462 whilst many studies now include estimates of bubble emissions of CH₄ e.g. (Bergen et al., 2019), the
463 necessary temporal resolution to accurately characterise ebullitive emission is not well established. The
464 finding here indicated that in such dynamic systems near continuous measurement is desirable and that
465 short term collection over one or two days could provide massive, over or underestimate of CH₄
466 ebullition.

467
468 Our results show very large temporal variation in emissions of all three gases, but in particular CO₂ and
469 CH₄, and this highlights the need for high frequency measurements to accurately characterize emissions
470 from lakes. Even the weekly frequency of the sampling in this study was not sufficient to directly measure
471 all the emission pathways and turnover flux had to be inferred from bottom water calculations. These data
472 show that to capture the extent of GHG emissions from lakes it is vital we include all forms of flux,
473 including ebullition and turnover flux. Recent work has highlighted the fact that most emissions of CH₄
474 (over 50%) from fresh waters come from highly variable systems (Rosentreter et al., 2021), with the mean
475 and median emission rates of CH₄ differing greatly, indicating a few large emitters are responsible for a
476 large proportion of emissions. The sampling frequency applied here is rare, if a more standard resolution
477 of monthly measurements was applied the emissions estimate of all the gases, but in particular CH₄,
478 would be highly dependent on what phase of the stratification was captured. As an example, a monthly
479 sampling frequency could potentially miss all the stratification peaks - consequently massively
480 underestimating emissions, whereas a different sampling frequency could catch a number of peaks and
481 give a much higher estimate. Thus, the same sampling frequency on the same lake, but timed differently
482 could lead to conclusions of highly variable emissions. Consequently, in these highly dynamic systems
483 where temporary stratification occur in summer, high frequency measurements are required to accurately
484 estimate emissions. This is possible through eddy covariance approaches capable of capturing short term

485 changes and covering a large area (Erkkilä et al., 2018) but the cost of these systems means they are not
486 scalable to many sites. An increasingly accessible alternative is the use of automatic flushing chambers
487 using low cost sensors (Bastviken et al., 2020), which provide the potential for affordable high spatial and
488 temporal resolution measurement of GHG dynamics. This is a requisite for understanding the drivers of
489 GHG dynamic, which is required for being able to predict how they will respond in a range of scenarios
490 related to land use, climate change and management interventions.

491

492 **Code/data availability**

493 The datasets generated during and/or analysed during the current study are not publicly available as they
494 form part of ongoing research projects but are available from the corresponding author on reasonable
495 request and will be made publicly available later in the research project.

496

497 **Author contributions**

498 MS secured the funding for the wider lake restoration research project supplying the data. TAD, MS and
499 JA conceptualized the gas study. TAD and AN established the buoy and sensor system. EL, CE, TAD,
500 TB and JA collected and analysed the data. TAD wrote the paper and all authors commented on earlier
501 versions and read and approved the final draft.

502 **Competing interests**

503 The authors declare that they have no conflicts of interest.

504

505 **Acknowledgement**

506 We thank our splendid technician team of Lene Vigh, Malene Kragh, Dorte Nedergaard and Dennis
507 Hansen for their extreme competence on the lab and the field. We acknowledge Theis Kragh for the depth
508 map of the lake already published in Søndergaard et al. 2023. We are very grateful to the Poul Due Jensen
509 Foundation for providing great support for this work and the Ormstrup project generally. TAD and CE
510 were also supported by GREENLAKES (No. 9040-00195B) and The European Union’s Horizon 2020
511 research and innovation programmes under grant agreement No 869296—The PONDERFUL Project.

512

513

514

515

516

517 Table 1. Summary lake information, summer mean values and (standard deviation) of a range of
518 variables

Variable	n	Year 2020
Secchi depth (m)	22	0.86 (0.28)
Chlorophyll a ($\mu\text{g/l}$)	20	53.4 (28.9)
pH	22	8.04 (0.77)
Total phosphorus (mg/l)	22	0.58 (0.11)
Total nitrogen (mg/l)	22	1.50 (0.41)

519

520 Table 2. Mean greenhouse gas flux (units CO_2 : $\text{mg CO}_2\text{-C m}^{-2} \text{ day}^{-1}$, N_2O : $\text{mg N}_2\text{O -N m}^{-2} \text{ day}^{-1}$, CH_4 both
521 diffusive and ebullitive in $\text{mg CH}_4\text{-C m}^{-2} \text{ day}^{-1}$) from the lake from spring to Autumn 2020. The emissions
522 are divided in diffusive, ebullitive emissions. The mean values for all the surface water stations and all
523 four transects of chambers are given. Emissions area separated into mixed versus stratified phases and
524 there SD are also given. Ebullition was collected for a period covering two weeks so on a number of
525 occasion covered both mixed and stratified periods thus ebullition has a third category where both
526 mixed and stratified conditions occurred is given. Ebullition was significantly different across the three
527 phases, diffusive fluxes were not significantly different for p values of 0.05.

528

529

530

Emission type	gas	mean	mixed	Stratified	Strat and mixed
Diffusive	CO ₂	493.7 <i>(529.6)</i>	559.6 <i>(433.1)</i>	449.8 <i>(587.6)</i>	
	CH ₄	9.47 <i>(16.0)</i>	5.9 <i>(4.1)</i>	12.7 <i>(20.2)</i>	
	N ₂ O	0.11 <i>(0.09)</i>	0.09 <i>(0.08)</i>	0.12 <i>(0.11)</i>	
Ebullition	CH ₄	17.28 <i>(19.62)</i>	4.84 <i>(3.44)</i>	47.29 <i>(21.95)</i>	12.74 <i>(10.34)</i>

531

532

533 Figure legends

534 Figure 1. Ormstrup lake bathymetry and sampling stations for surface water greenhouse gas sampling
535 (St1, St2, St3) bottom waters were sampled at S3. Transects of 10 bubble traps were placed on T1- T4.

536 Adapted from the Søndergaard et al. 2023.

537 Figure 2 Temperature profile from June 2020 when the buoy was deployed and surface and bottom water
538 oxygen from June to the end of September 2020. Manual chlorophyll-a ($\mu\text{g L}^{-1}$) values are also given in
539 the top panel.

540 Figure 3. Dissolved CH_4 concentrations from surface and bottom waters – thermal stratification periods
541 highlighted in grey and the white background indicate mixed waters

542 Figure 4 . Dissolved CO_2 concentrations from surface and bottom waters–thermal stratification periods
543 highlighted in grey and the white background indicate mixed waters

544 Figure 5 Dissolved N_2O gas concentrations surface and bottom thermal stratification periods highlighted
545 in grey and the white background indicate mixed waters

546 Figure 6. Ormstrup lake surface fluxes of the CH_4 , CO_2 and N_2O gases based on dissolved concentration ,
547 thermal stratification periods highlighted in grey and the white background indicate mixed waters

548 Figure 7. Plot of CH_4 ebullition averaged for each transect (10 chambers per transect), data collected from
549 40 traps every two weeks. Thermal stratification periods highlighted in grey and the white background
550 indicate mixed waters.

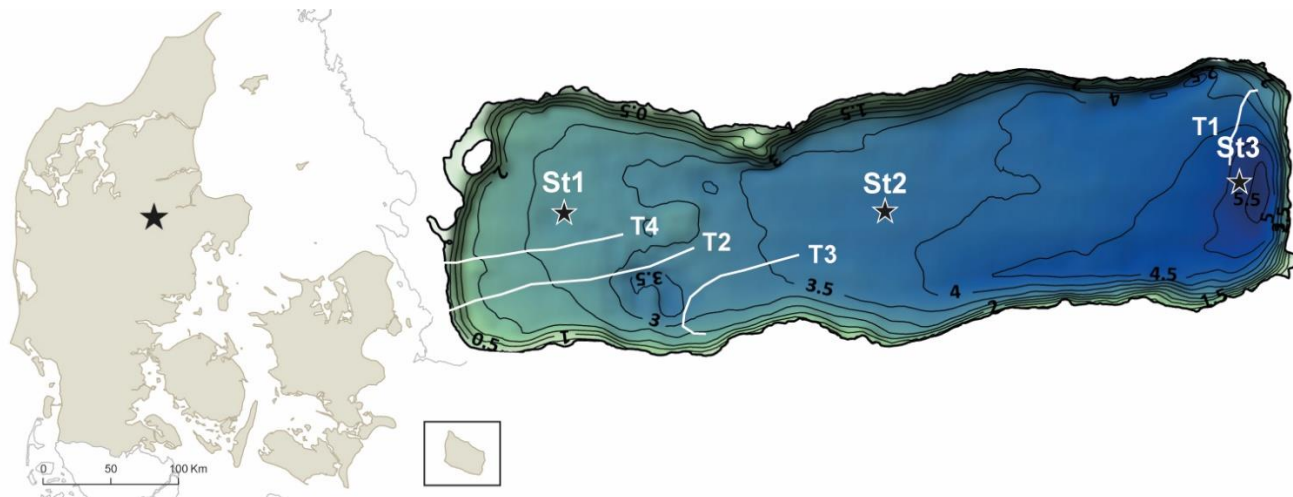
551 Figure 8 – Total lake emissions per gas over the growing season in CO_2 equivalents. The emissions are
552 divided different emission modes: Diffusive, ebullitive and turnover flux. All estimates contain some
553 uncertainty, in particular ebullitive flux is an underestimate and the turnover flux also contains a great deal
554 of uncertainty.

555 Figure 9. Summary of the quantities of the gases present in the water and the volumes emitted from the
556 different pathways. The size of the arrow is proportional to the emissions from each pathway and with the
557 stratified state on the left and the mixed state on the right, with the turnover flux in the centre.

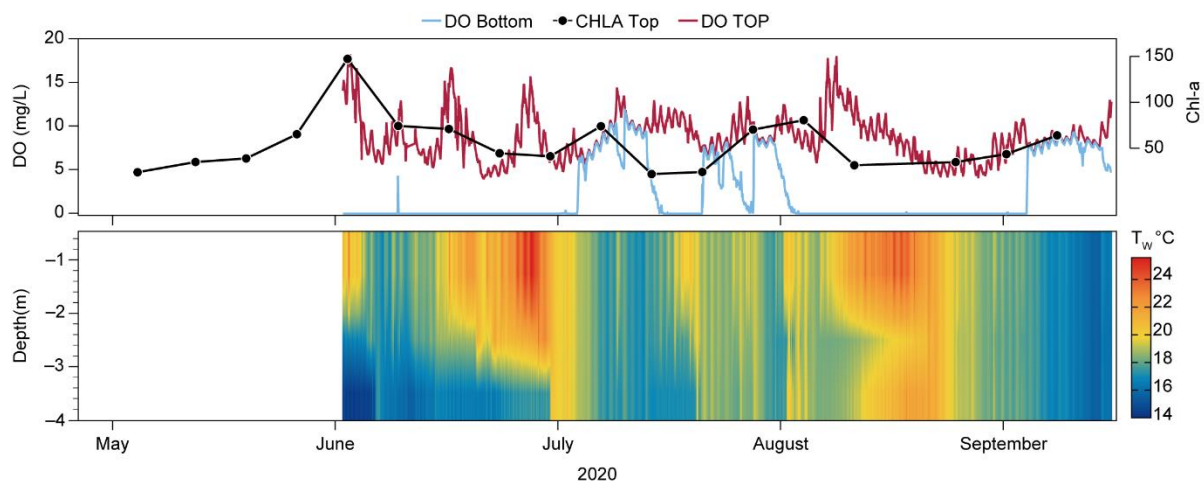
558

559 Figures and legends

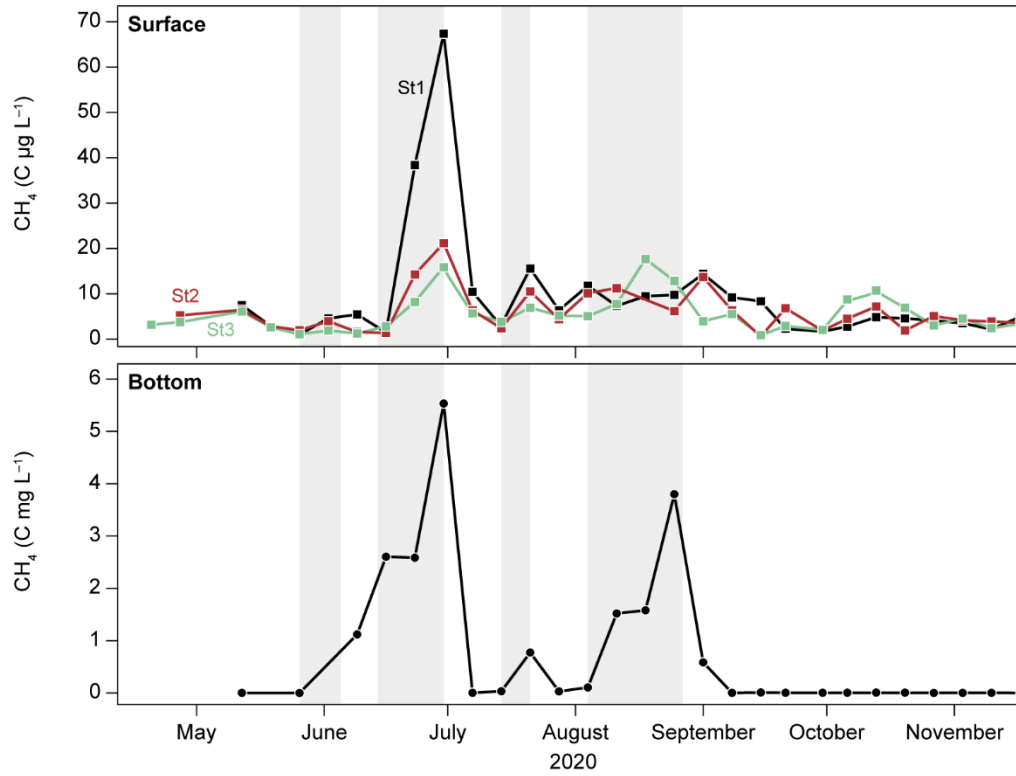
560 Figure 1.



561
562 Figure 1. Ormstrup lake bathymetry and sampling stations for surface water greenhouse gas sampling (S1,
563 S2, S3) bottom waters were sampled at S3. Transects of 10 bubble traps were placed on T1- T4. Adapted
564 from the Søndergaard et al. 2023.
565



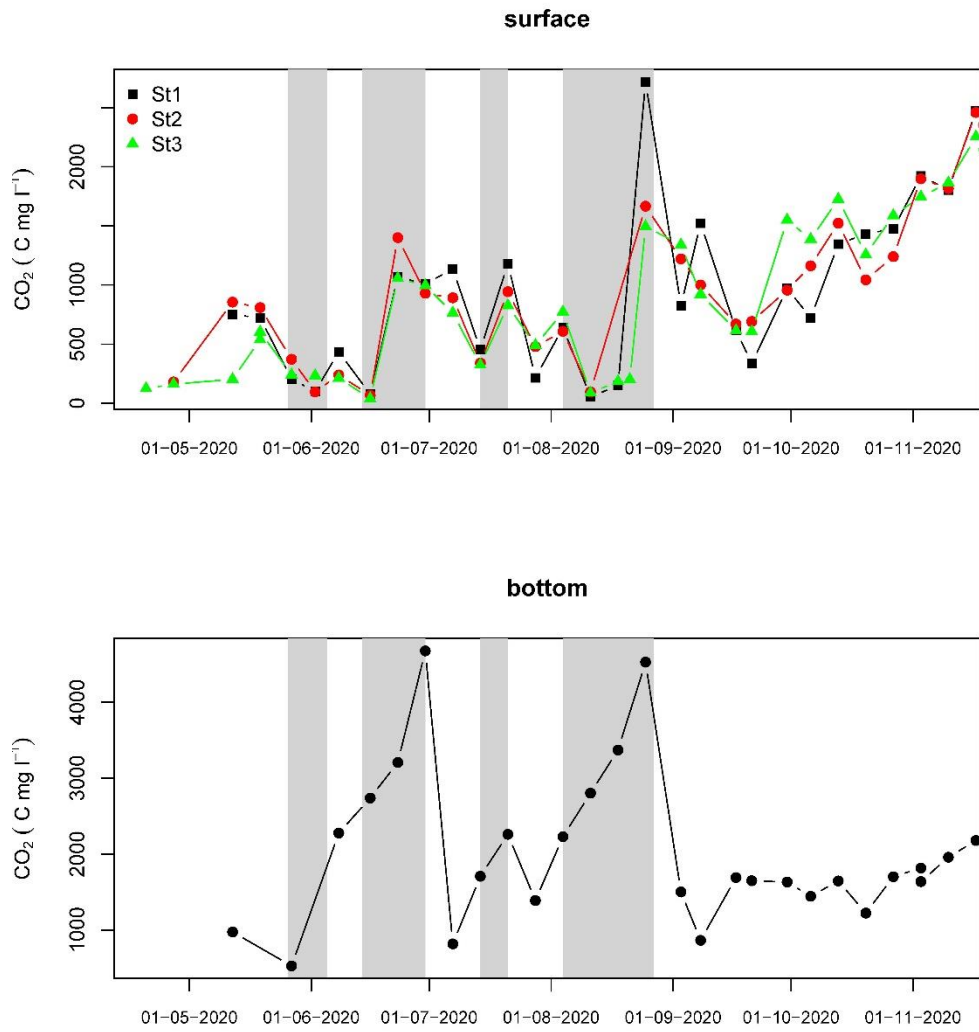
566
567 Figure 2 Temperature profile from June when the buoy was deployed and surface and bottom water
568 oxygen from June to the end of September. Chlorophyll-a ($\mu\text{g L}^{-1}$) values are also given in the top panel
569 and surface (DO TOP) and bottom (DO Bottom) dissolved oxygen (mg L^{-1}) are also given
570



571

572 Figure 3. Dissolved CH₄ concentrations from surface and bottom waters – thermal stratification periods

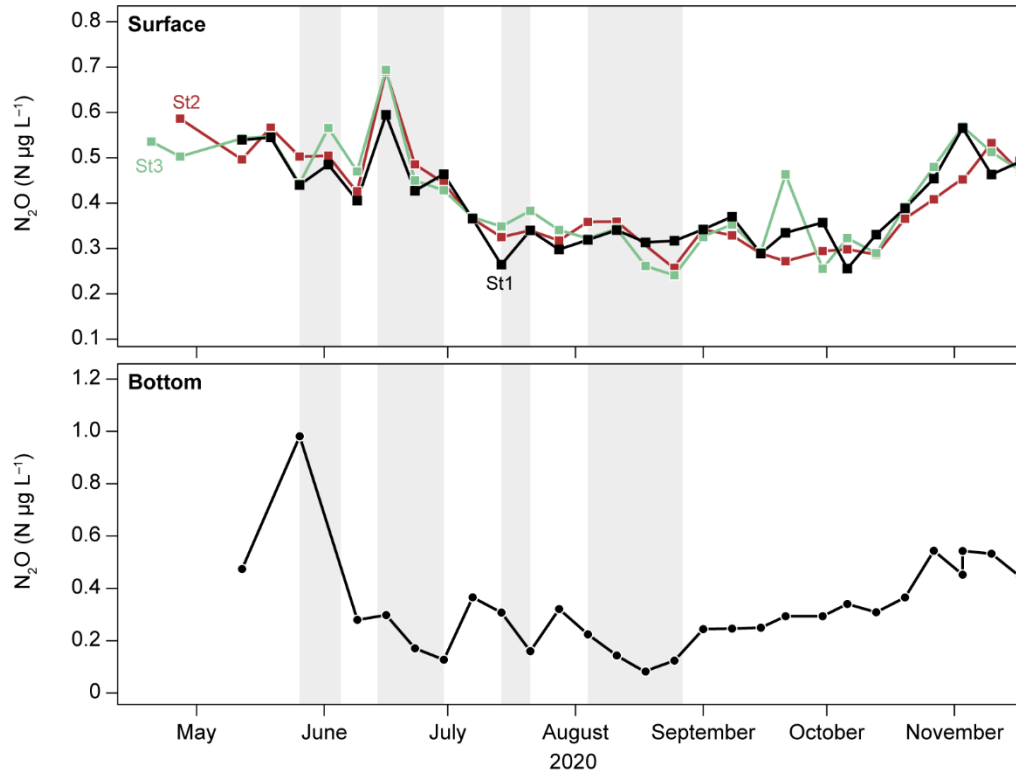
573 highlighted in grey; white background indicate mixed waters. Note different y axis scales



574

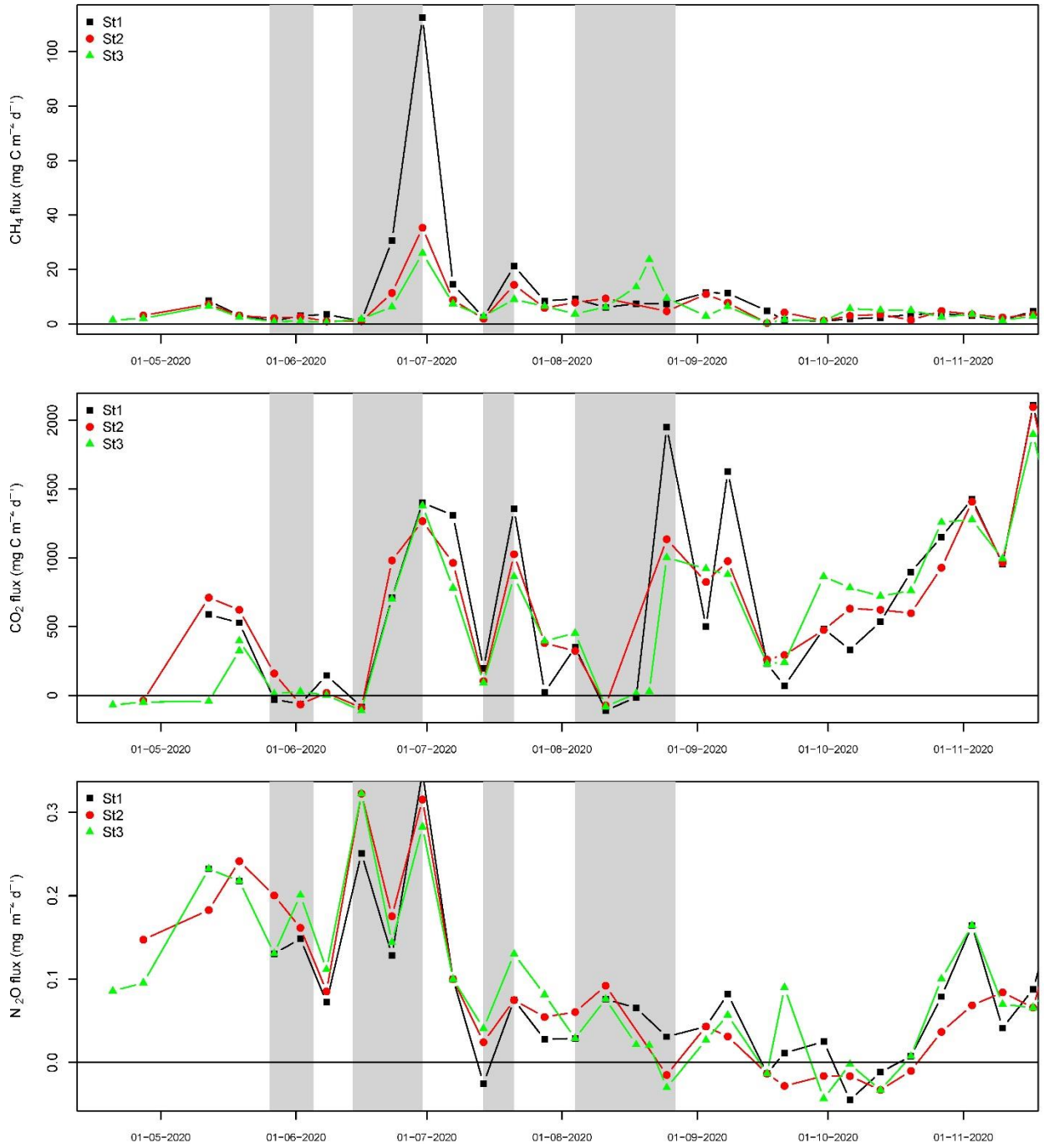
575 Figure 4 . Dissolved CO₂ concentrations from surface and bottom waters–

576 thermal stratification periods highlighted in grey; white background indicate mixed waters



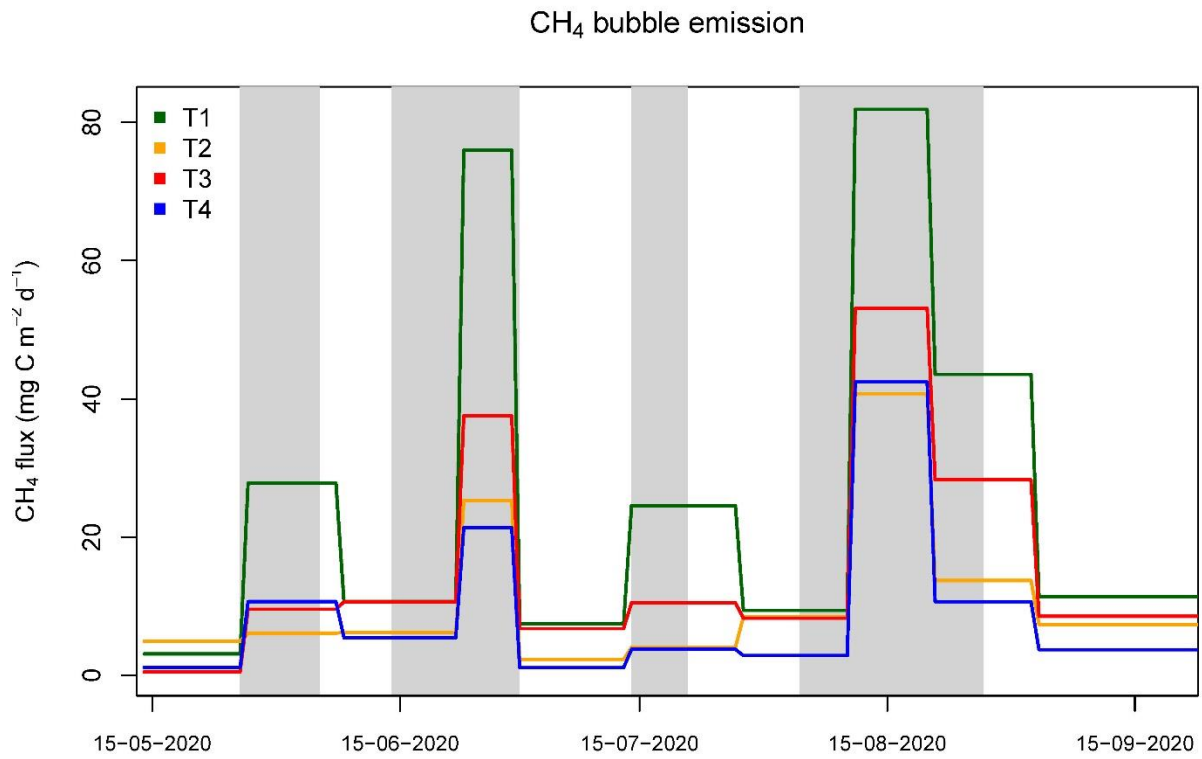
577

578 Figure 5 Dissolved N_2O gas concentrations surface and bottom thermal stratification periods highlighted
 579 in grey; white background indicate mixed waters



580
 581 Figure 6. Omstrup lakesurface fluxes of the CH₄, CO₂ and N₂O gases based on dissolved concentration ,
 582 thermal stratification periods highlighted in grey; white background indicate mixed waters
 583

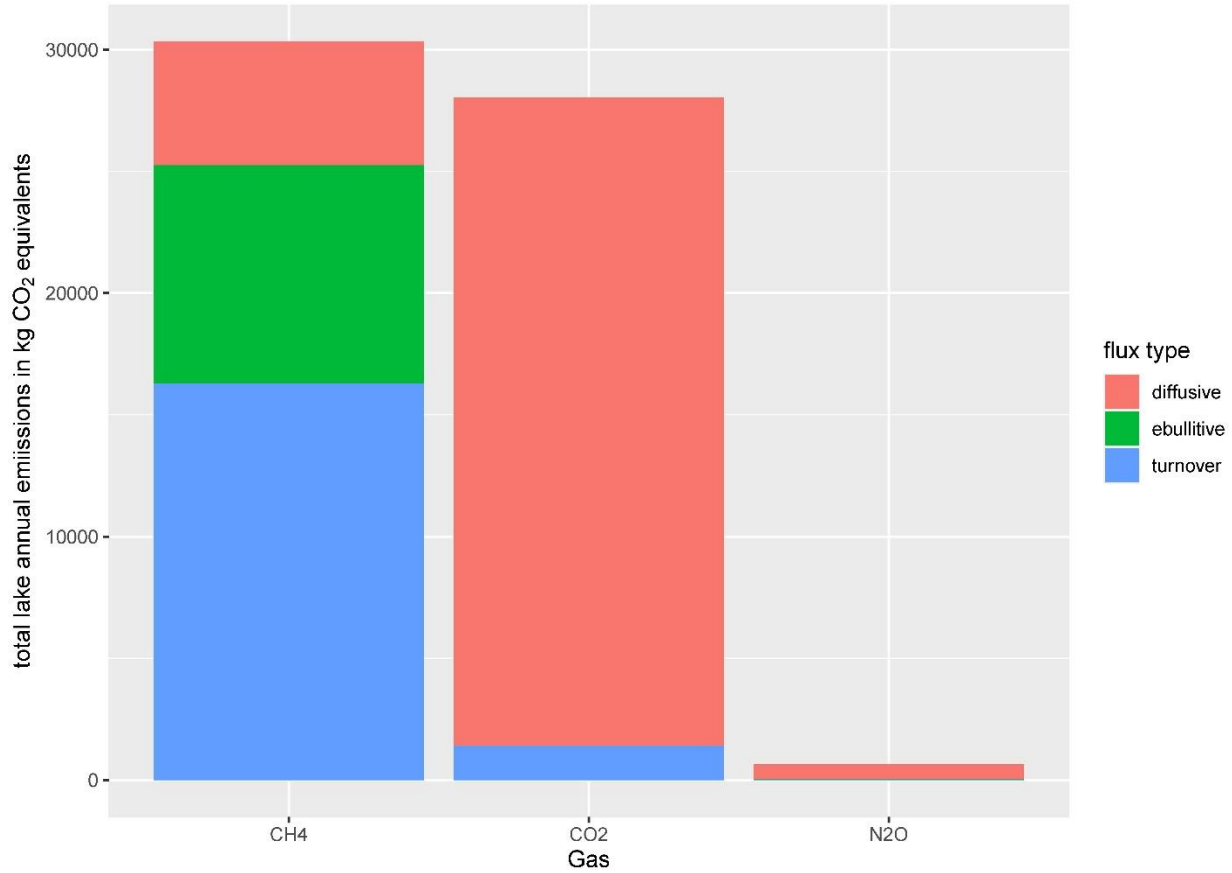
584



585

586 Figure 7. Plot of CH₄ ebullition averaged for each transect (10 chambers per transect), data collected from
587 40 traps every two weeks. thermal stratification periods highlighted in grey; white background indicate
588 mixed waters.

589

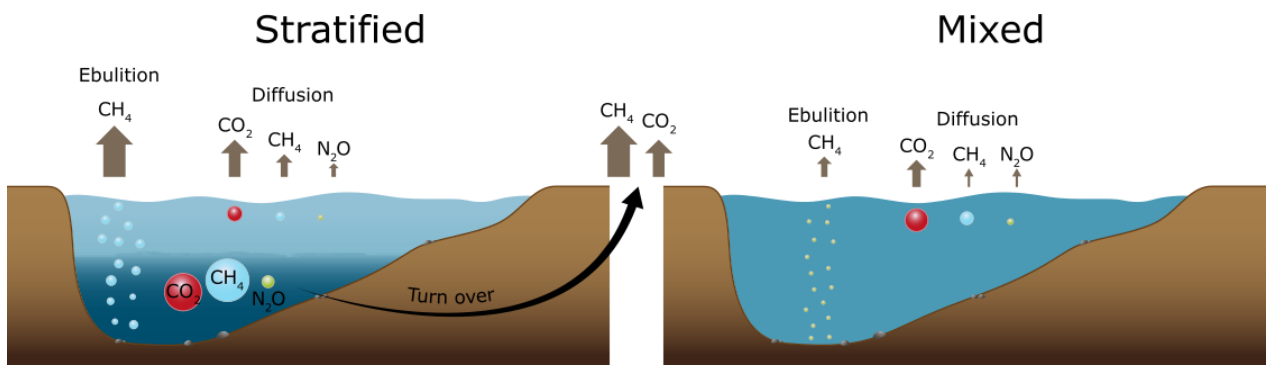


590

591 Figure 8 – Total lake emissions per gas over the growing season in CO₂ equivalents. The emissions are
 592 divided different emission pathways: Diffusive, ebullitive and turnover flux.

593

594



595

596 Figure 9 Summary of different flux types (bubble, diffusive and turnover) for the main greenhouse gases
 597 (CH₄ CO₂ and N₂O) observed between the stratified and mixed phases at Ormstrup lake patterns in the
 598 stratified and mixed phase. The turnover flux of CH₄ and CO₂ is also represented. The size of the arrow

599 represents the relative amount of emission and the size of the circle in the lake represents the
600 concentration of dissolved gases in stratified or mixed water column.

601

602

603 **References**

604 Aben, R. C. H., Barros, N., van Donk, E., Frenken, T., Hilt, S., Kazanjian, G., Lamers, L. P. M., Peeters, E. T.
605 H. M., Roelofs, J. G. M., de Senerpont Domis, L. N., Stephan, S., Velthuis, M., Van de Waal, D. B., Wik, M.,
606 Thornton, B. F., Wilkinson, J., DelSontro, T., and Kosten, S.: Cross continental increase in methane
607 ebullition under climate change, *Nat. Comms.*, 8, 1682, <https://doi.org/10.1038/s41467-017-01535-y>,
608 2017.

609 Audet, J., Carstensen, M. V., Hoffmann, C. C., Lavaux, L., Thiemer, K., and Davidson, T. A.: Greenhouse
610 gas emissions from urban ponds in Denmark, *Inland Waters*, 1-13,
611 <https://doi.org/10.1080/20442041.2020.1730680>, 2020.

612 Bartosiewicz, M., Laurion, I., and MacIntyre, S.: Greenhouse gas emission and storage in a small shallow
613 lake, *Hydrobiologia*, 757, 101-115, <https://doi.org/10.1007/s10750-015-2240-2>, 2015.

614 Bartosiewicz, M., Laurion, I., Clayer, F., and Maranger, R.: Heat-Wave Effects on Oxygen, Nutrients, and
615 Phytoplankton Can Alter Global Warming Potential of Gases Emitted from a Small Shallow Lake, *Environ.*
616 *Sci. Technol.*, 50, 6267-6275, <https://pubs.acs.org/doi/10.1021/acs.est.5b06312>, 2016.

617 Bartosiewicz, M., Przytulska, A., Lapierre, J.-F., Laurion, I., Lehmann, M. F., and Maranger, R.: Hot tops,
618 cold bottoms: Synergistic climate warming and shielding effects increase carbon burial in lakes, *Limnol.*
619 *Oceanogr. Lett.*, 4, 132-144, <https://doi.org/10.1002/lo.10117>, 2019.

620 Bastviken, D., Cole, J. J., Pace, M. L., and Van de Bogert, M. C.: Fates of methane from different lake
621 habitats: Connecting whole-lake budgets and CH₄ emissions, *J. Geophys. Res.*, 113, G02024,
622 <https://doi.org/10.1029/2007JG000608>, 2008.

623 Bastviken, D., Nygren, J., Schenk, J., Parellada Massana, R., and Duc, N. T.: Technical note: Facilitating the
624 use of low-cost methane (CH₄) sensors in flux chambers – calibration, data processing, and an open-
625 source make-it-yourself logger, *Biogeosciences*, 17, 3659-3667, [https://doi.org/10.5194/bg-17-3659-](https://doi.org/10.5194/bg-17-3659-2020)
626 [2020](https://doi.org/10.5194/bg-17-3659-2020), 2020.

627 Bastviken, D., Sundgren, I., Natchimuthu, S., Reyier, H., and Gålfalk, M.: Technical Note: Cost-efficient
628 approaches to measure carbon dioxide fluxes and concentrations in terrestrial and aquatic
629 environments using mini loggers, *Biogeosciences*, 12, 3849-3859,
630 <https://doi.org/10.5194/bg-12-3849-2015>, 2015.

631 Bastviken, D., Treat, C. C., Pangala, S. R., Gauci, V., Enrich-Prast, A., Karlson, M., Gålfalk, M., Romano, M.
632 B., and Sawakuchi, H. O.: The importance of plants for methane emission at the ecosystem scale, *Aquat.*
633 *Bot.*, 184, 103596, <https://doi.org/10.1016/j.aquabot.2022.103596>, 2023.

634 Beaulieu, J. J., DelSontro, T., and Downing, J. A.: Eutrophication will increase methane emissions from
635 lakes and impoundments during the 21st century, *Nat. Comms.*, 10, 1-5,
636 <https://doi.org/10.1038/s41467-019-09100-5>, 2019.

637 Bergen, T. J. H. M., Barros, N., Mendonça, R., Aben, R. C. H., Althuisen, I. H. J., Huszar, V., Lamers, L. P.
638 M., Lürling, M., Roland, F., and Kosten, S.: Seasonal and diel variation in greenhouse gas emissions from
639 an urban pond and its major drivers, *Limnol. Oceanogr.*, 64, 2129-2139,
640 <https://doi.org/10.1002/lno.11173>, 2019.

641 Blees, J., Niemann, H., Wenk, C. B., Zopfi, J., Schubert, C. J., Kirf, M. K., Veronesi, M. L., Hitz, C., and
642 Lehmann, M. F.: Micro-aerobic bacterial methane oxidation in the chemocline and anoxic water column
643 of deep south-Alpine Lake Lugano (Switzerland), *Limnol. Oceanogr.*, 59, 311-324,
644 <https://doi.org/10.4319/lo.2014.59.2.0311>, 2014.

645 Burke, S. A., Wik, M., Lang, A., Contosta, A. R., Palace, M., Crill, P. M., and Varner, R. K.: Long-Term
646 Measurements of Methane Ebullition From Thaw Ponds, *J. Geophys. Res. Biogeosci.* . 124, 2208-2221,
647 <https://doi.org/10.1029/2018JG004786>, 2019.

648 Cole, J.: Freshwater in flux, *Nat. Geosci.*, 6, 13-14, <https://doi.org/10.1038/ngeo1696>, 2013.

649 Cole, J. J. and Caraco, N. F.: Atmospheric exchange of carbon dioxide in a low-wind oligotrophic lake
650 measured by the addition of SF₆, *Limnol. Oceanogr.*, 43, 647-656,
651 <https://doi.org/10.4319/lo.1998.43.4.0647>, 1998.

652 Davidson, T. A., Audet, J., Jeppesen, E., Landkildehus, F., Lauridsen, T. L., Søndergaard, M., and
653 Syvaranta, J.: Synergy between nutrients and warming enhances methane ebullition from experimental
654 lakes, *Nat. Clim. Chang.*, 8, 156-160, <https://doi.org/10.1038/s41558-017-0063-z>, 2018.

655 Davidson, T. A., Audet, J., Svenning, J.-C. C., Lauridsen, T. L., Søndergaard, M., Landkildehus, F., Larsen, S.
656 E., and Jeppesen, E.: Eutrophication effects on greenhouse gas fluxes from shallow-lake mesocosms
657 override those of climate warming, *Glob. Chang. Biol.*, 21, 4449-4463,
658 <https://doi.org/10.1111/gcb.13062>, 2015.

659 Deacon, E. L.: Sea-air gas transfer: The wind speed dependence, *Bound.- Layer. Meteorol.*, 21, 31-37,
660 <https://doi.org/10.1007/bf00119365>, 1981.

661 Deemer, B. R. and Holgerson, M. A.: Drivers of Methane Flux Differ Between Lakes and Reservoirs,
662 Complicating Global Upscaling Efforts, *J. Geophys. Res. Biogeosci.* . 126, e2019JG005600,
663 <https://doi.org/10.1029/2019JG005600>, 2021.

664 DelSontro, T., Boutet, L., St-Pierre, A., del Giorgio, P. A., and Prairie, Y. T.: Methane ebullition and
665 diffusion from northern ponds and lakes regulated by the interaction between temperature and system
666 productivity, *Limnol. Oceanogr.*, 61, S62-S77, <http://doi.wiley.com/10.1002/lno.10335>, 2016.

667 Erkkilä, K. M., Ojala, A., Bastviken, D., Biermann, T., Heiskanen, J. J., Lindroth, A., Peltola, O., Rantakari,
668 M., Vesala, T., and Mammarella, I.: Methane and carbon dioxide fluxes over a lake: comparison between
669 eddy covariance, floating chambers and boundary layer method, *Biogeosciences*, 15, 429-445,
670 10.5194/bg-15-429-2018, 2018.

671 Esposito, C., Nijman, T. P. A., Veraart, A. J., Audet, J., Levi, E. E., Lauridsen, T. L., and Davidson, T. A.:
672 Activity and abundance of methane-oxidizing bacteria on plants in experimental lakes subjected to
673 different nutrient and warming treatments, *Aquat. Bot.*, 185, 103610,
674 <https://doi.org/10.1016/j.aquabot.2022.103610>, 2023.

675 Holgerson, M. A. and Raymond, P. A.: Large contribution to inland water CO₂ and CH₄ emissions from
676 very small ponds, *Nat. Geosci.*, 9, 222-226, 2016.

677 Holgerson, M. A., Richardson, D. C., Roith, J., Bortolotti, L. E., Finlay, K., Hornbach, D. J., Gurung, K., Ness,
678 A., Andersen, M. R., Bansal, S., Finlay, J. C., Cianci-Gaskill, J. A., Hahn, S., Janke, B. D., McDonald, C.,
679 Mesman, J. P., North, R. L., Roberts, C. O., Sweetman, J. N., and Webb, J. R.: Classifying Mixing Regimes
680 in Ponds and Shallow Lakes, *Water Resour. Res.*, 58, e2022WR032522,
681 <https://doi.org/10.1029/2022WR032522>, 2022.

682 Jespersen, A. and Christoffersen, K.: Measurements of Chlorophyll a from phytoplankton using ethanol
683 as extraction solvent., *Archiv für Hydrobiologie*, 109, 445-454, 1987.

684 Kirillin, G. and Shatwell, T.: Generalized scaling of seasonal thermal stratification in lakes, *Earth Sci. Rev.*,
685 161, 179-190, <https://doi.org/10.1016/j.earscirev.2016.08.008>, 2016.

686 Koschorreck, M., Prairie, Y. T., Kim, J., and Marcé, R.: Technical note: CO₂ is not like CH₄ – limits of and
687 corrections to the headspace method to analyse pCO₂ in fresh water, *Biogeosciences*, 18, 1619-1627,
688 10.5194/bg-18-1619-2021, 2021.

689 McAuliffe, C.: Gas chromatographic determination of solutes by multiple phase equilibrium, *Chem*
690 *Technol*, 1, 46-51, 1971.

691 Meerhoff, M., Audet, J., Davidson, T. A., De Meester, L., Hilt, S., Kosten, S., Liu, Z., Mazzeo, N., Paerl, H.,
692 Scheffer, M., and Jeppesen, E.: Feedbacks between climate change and eutrophication: revisiting the
693 allied attack concept and how to strike back, *Inland Waters*, 1-42,
694 <https://doi.org/10.1080/20442041.2022.2029317>, 2022.

695 Peacock, M., Audet, J., Jordan, S., Smeds, J., and Wallin, M. B.: Greenhouse gas emissions from urban
696 ponds are driven by nutrient status and hydrology, *Ecosphere*, 10, e02643,
697 <https://doi.org/10.1002/ecs2.2643>, 2019.

698 Peacock, M., Audet, J., Bastviken, D., Cook, S., Evans, C. D., Grinham, A., Holgerson, M. A., Högbom, L.,
699 Pickard, A. E., Zieliński, P., and Futter, M. N.: Small artificial waterbodies are widespread and persistent
700 emitters of methane and carbon dioxide, *Glob. Chang. Biol.*, 27, 5109-5123,
701 <https://doi.org/10.1111/gcb.15762>, 2021.

702 Petersen, S. O., Hoffmann, C. C., Schäfer, C. M., Blicher-Mathiesen, G., Elsgaard, L., Kristensen, K.,
703 Larsen, S. E., Torp, S. B., and Greve, M. H.: Annual emissions of CH₄ and N₂O, and ecosystem respiration,
704 from eight organic soils in Western Denmark managed by agriculture, *Biogeosciences*, 9, 403-422,
705 <https://doi.org/10.5194/bg-9-403-2012>, 2012.

706 Pinheiro, J., Bates, D., DebRoy, S., Sarkar, D., and R Core Team: *nlme: Linear and Nonlinear Mixed Effects*
707 *Models*, 2014.

708 R Development Core Team: *R: a language and environment for statistical computing*. R Foundation for
709 Statistical Computing (4.2.1) [code], 2022.

710 Ray, N. E. and Holgerson, M. A.: High Intra-Seasonal Variability in Greenhouse Gas Emissions From
711 Temperate Constructed Ponds, *Geophysical Research Letters*, 50, e2023GL104235,
712 <https://doi.org/10.1029/2023GL104235>, 2023.

713 Rosentreter, J. A., Borges, A. V., Deemer, B. R., Holgerson, M. A., Liu, S., Song, C., Melack, J., Raymond, P.
714 A., Duarte, C. M., Allen, G. H., Olefeldt, D., Poulter, B., Battin, T. I., and Eyre, B. D.: Half of global methane
715 emissions come from highly variable aquatic ecosystem sources, *Nat. Geosci.*, 14, 225-230,
716 <https://doi.org/10.1038/s41561-021-00715-2>, 2021.

717 Saarela, T., Rissanen, A. J., Ojala, A., Pumpanen, J., Aalto, S. L., Tirola, M., Vesala, T., and Jäntti, H.: CH₄
718 oxidation in a boreal lake during the development of hypolimnetic hypoxia, *Aquat. Sci.*, 82, 19,
719 <https://doi.org/10.1007/s00027-019-0690-8>, 2019.

720 Schubert, C. J., Diem, T., and Eugster, W.: Methane Emissions from a Small Wind Shielded Lake
721 Determined by Eddy Covariance, Flux Chambers, Anchored Funnels, and Boundary Model Calculations: A
722 Comparison, *Environ. Sci. Technol.*, 46, 4515-4522, <https://doi.org/10.1021/es203465x>, 2012.

723 Sørensen, J. S., Sand-Jensen, K., Martinsen, K. T., Polauke, E., Kjær, J. E., Reitzel, K., and Kragh, T.: Methane and
724 carbon dioxide fluxes at high spatiotemporal resolution from a small temperate lake, *Sci. Total Environ.*,
725 878, 162895, <https://doi.org/10.1016/j.scitotenv.2023.162895>, 2023.

726 Søndergaard, M., Jeppesen, E., Peder Jensen, J., and Lildal Amsinck, S.: Water Framework Directive:
727 ecological classification of Danish lakes, *J. Appl. Ecol.*, 42, 616-629, <https://doi.org/10.1111/j.1365-2664.2005.01040.x>, 2005.

728 Søndergaard, M., Nielsen, A., Johansson, L. S., and Davidson, T. A.: Temporarily summer-stratified lakes
729 are common: profile data from 436 lakes in lowland Denmark, *Inland Waters*, 1-14,
730 10.1080/20442041.2023.2203060, 2023a.

731 Søndergaard, M., Nielsen, A., Skov, C., Baktoft, H., Reitzel, K., Kragh, T., and Davidson, T. A.: Temporarily
732 and frequently occurring summer stratification and its effects on nutrient dynamics, greenhouse gas
733 emission and fish habitat use: case study from Lake Ormstrup (Denmark), *Hydrobiologia*, 850, 65-79,
734 <https://doi.org/10.1007/s10750-022-05039-9>, 2023b.

735 Thottathil, S. D., Reis, P. C. J., and Prairie, Y. T.: Methane oxidation kinetics in northern freshwater lakes,
736 *Biogeochemistry*, 143, 105-116, 10.1007/s10533-019-00552-x, 2019.

737 Wanninkhof, R.: Relationship between wind-speed and gas-exchange over the ocean, *J. Geophys. Res.*
738 *Oceans*, 97, 7373-7382, <https://doi.org/10.1029/92jc00188>, 1992.

739 Weiss, R. F.: Carbon dioxide in water and seawater: the solubility of a non-ideal gas, *Mar. Chem.*, 2, 203-
740 215, [https://doi.org/10.1016/0304-4203\(74\)90015-2](https://doi.org/10.1016/0304-4203(74)90015-2), 1974.

742 Weiss, R. F. and Price, B. A.: Nitrous oxide solubility in water and seawater, *Mar. Chem.*, 8, 347-359,
743 [https://doi.org/10.1016/0304-4203\(80\)90024-9](https://doi.org/10.1016/0304-4203(80)90024-9), 1980.

744 West, W. E., Coloso, J. J., and Jones, S. E.: Effects of algal and terrestrial carbon on methane production
745 rates and methanogen community structure in a temperate lake sediment, *Freshw. Biol.*, 57, 949-955,
746 <https://doi.org/10.1111/j.1365-2427.2012.02755.x>, 2012.

747 Wiesenburg, D. A. and Guinasso, N. L.: Equilibrium solubilities of methane, carbon monoxide, and
748 hydrogen in water and sea water, *J. Chem. Eng. Data* . 24, 356-360,
749 <https://doi.org/10.1021/je60083a006>, 1979.

750 Wik, M., Crill, P. M., Varner, R. K., and Bastviken, D.: Multiyear measurements of ebullitive methane flux
751 from three subarctic lakes, *J. Geophys. Res. Biogeosci.* . 118, 1307–1321,
752 <https://doi.org/10.1002/jgrg.20103>, 2013.

753 Winslow, L., Read, J., Woolway, I., Brenttrup, J., Leach, T., Zwart, J., Albers, S., and Collinge, D.:
754 rLakeAnalyzer: Lake Physics Tools: R package (1.11.4.1) [code], 2019.

755 Woolway, R. I. and Merchant, C. J.: Worldwide alteration of lake mixing regimes in response to climate
756 change, *Nat. Geosci.*, 12, 271-276, <https://doi.org/10.1038/s41561-019-0322-x>, 2019.

757 Yvon-Durocher, G., Allen, A. P., Montoya, J. M., Trimmer, M., and Woodward, G.: The temperature
758 dependence of the carbon cycle in aquatic ecosystems, *Adv. Ecol. Res.*, 43, 267-313,
759 <https://doi.org/10.1016/B978-0-12-385005-8.00007-1>, 2010.

760 Yvon-Durocher, G., Allen, A. P., Bastviken, D., Conrad, R., Gudas, C., St-Pierre, A., Thanh-Duc, N., and del
761 Giorgio, P. A.: Methane fluxes show consistent temperature dependence across microbial to ecosystem
762 scales, *Nature*, 507, 488-491, <https://doi.org/10.1038/nature13164>, 2014.

763 Zhou, Y., Zhou, L., Zhang, Y., de Souza, J. G., Podgorski, D. C., Spencer, R. G. M., Jeppesen, E., and
764 Davidson, T. A.: Autochthonous dissolved organic matter potentially fuels methane ebullition from
765 experimental lakes, *Water Res.*, 166, 115048, <https://doi.org/10.1016/j.watres.2019.115048>, 2019.

766